EPJ A
Hadrons and Nuclei
EPJ.org
your physics journal

Eur. Phys. J. A (2015) **51**: 54 DOI 10.1140/epja/i2015-15054-7

Study of lifetimes of low-lying levels in ^{53}Mn

K.P. Singh, Mumtaz Oswal, B.R. Behera, Ashok Kumar and Gulzar Singh

Società Italiana di Fisica
Springer

Eur. Phys. J. A (2015) **51**: 54
DOI 10.1140/epja/i2015-15054-7

THE EUROPEAN PHYSICAL JOURNAL A

Regular Article – Experimental Physics

Study of lifetimes of low-lying levels in ^{53}Mn

K.P. Singh[a], Mumtaz Oswal, B.R. Behera, Ashok Kumar, and Gulzar Singh

Cyclotron Laboratory, Department of Physics, Centre of Advance Study in Physics, Panjab University, Chandigarh-160014, India

Received: 16 October 2014 / Revised: 3 March 2015
Published online: 12 May 2015 – © Società Italiana di Fisica / Springer-Verlag 2015
Communicated by C. Broggini

Abstract. The properties of low-lying states of ^{53}Mn were investigated via the ^{53}Cr(p, nγ)^{53}Mn reaction using 4.3 MeV proton beam energy. The lifetimes of the levels at 1289.5, 1440.8, 1620.0 and 2273.8 keV excitation energies were measured using the Doppler Shift Attenuation Method (DSAM). The reduced transition probabilities $B(M1)$ and $B(E2)$ were extracted using the measured values of lifetimes for these levels and the mixing ratios from the literature. These values are compared with already known experimental values as well as the shell model calculations using an effective interaction.

1 Introduction

The ^{53}Mn nucleus has been extensively investigated in the past years via EC-decay [1], light particle reactions [2–16] and heavy ion reactions [17–19]. The available experimental information on this nucleus has been compiled by Huo Junde [20]. The structure of the fp shell nuclei, at or near the neutron shell closure $N = 28$, has been studied using the shell model calculation [21,22]. Hitoshi *et al.* [23] have also studied the energy levels and electromagnetic properties of ^{53}Mn in terms of large-scale shell model calculations.

The study of ^{53}Mn is a continuation of our previous work [24,25] for lifetime measurements of low-energy nuclear states in the mass region of $A < 100$. Preliminary results on lifetimes in ^{53}Mn have already been presented in a conference [26]. The aim of the present investigation was to provide further experimental information about the low-lying levels of ^{53}Mn nucleus through (p, nγ) reaction using an improved detection system. In this work we have measured the lifetimes of the low-lying states using the Doppler Shift Attenuation (DSA) technique. The branching ratios for various transitions were also measured from the γ-ray spectra recorded at 55°. The reduced transition probabilities $B(M1)$ and $B(E2)$ were obtained from our measured lifetimes and branching ratios and the mixing ratios reported in the literature [9,20]. The new experimental results are compared with the predictions of the shell model using an effective interaction.

[a] e-mail: singhkp@pu.ac.in

2 Experimental procedure

A thick self-supporting pellet of spectroscopically enriched (96%) ^{53}Cr of thickness about 100 mg/cm^2 was bombarded with a 4.3 MeV energy proton beam to excite the levels of ^{53}Mn through ^{53}Cr(p, nγ)^{53}Mn reaction (Q-value = −1.38 MeV). The target was placed at an angle of 45° with respect to the beam direction.

The singles gamma-ray spectra were measured at 0°, 30°, 45°, 75°, and 90° w.r.t. beam direction. The gamma-ray spectra were detected at a distance of 8.8 cm from the target with a 70 cm^3 coaxial HPGe detector with a resolution of 1.9 keV for the 1332 keV line of ^{60}Co. A typical gamma-ray spectrum acquired with the detector at 90° is shown in fig. 1. The other experimental set-up details are given in our previous publications [24,25] and references therein.

3 Data analysis and results

The gamma-ray spectra were analysed using the computer code PEAKFIT [27]. In the spectrum of fig. 1, the peaks due to gamma-rays not belonging to ^{53}Mn are marked with their respective sources. The ^{27}Al peaks in the spectrum are due to the Aluminum collimator in front of the detector. The present level scheme at low excitation for ^{53}Mn as shown in fig. 2 confirms the previously reported level scheme [20]. The gamma-ray energies and branching ratios measured in the present work along with previously reported values [9,11,28] are given in table 1. The mean

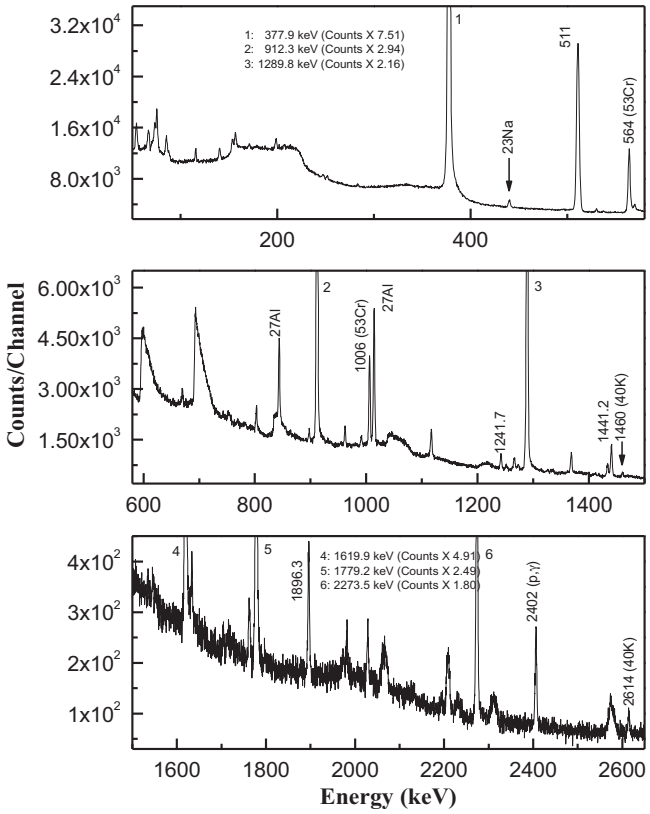

Fig. 1. A typical gamma-ray spectrum detected at 90° from the ^{53}Cr(p, nγ)^{53}Mn reaction at 4.3 MeV proton beam energy.

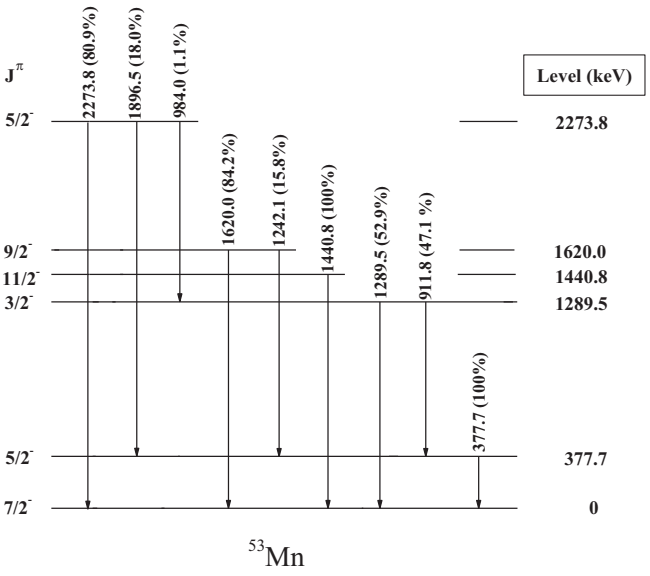

Fig. 2. The level scheme of low-lying levels in ^{53}Mn [20]. The reported branching ratios have been measured in the present work.

Table 1. Level energies, gamma-ray energies and branching ratios in ^{53}Mn.

Level	Gamma-ray	Branching ratios			
(keV)	(keV)	Present	Ref. [9]	Ref. [11]	Ref. [28]
377.7	377.7	100	100		100
1289.5	911.8	47.1 ± 0.2	49 ± 1	44 ± 3	51
	1289.5	52.9 ± 0.4	51 ± 1	56 ± 3	49
1440.8	1440.8	100	100		100
1620.0	1242.1	15.8 ± 1.8	10[(a)]	10 ± 2	17
	1620.0	84.2 ± 2.0	90[(a)]	90 ± 2	83
2273.8	984.0	1.1 ± 0.4			
	1896.5	18.0 ± 1.2	26 ± 3		26
	2273.8	80.9 ± 2.2	74 ± 6		74

[(a)] Values based on relative peak areas at 90° only.

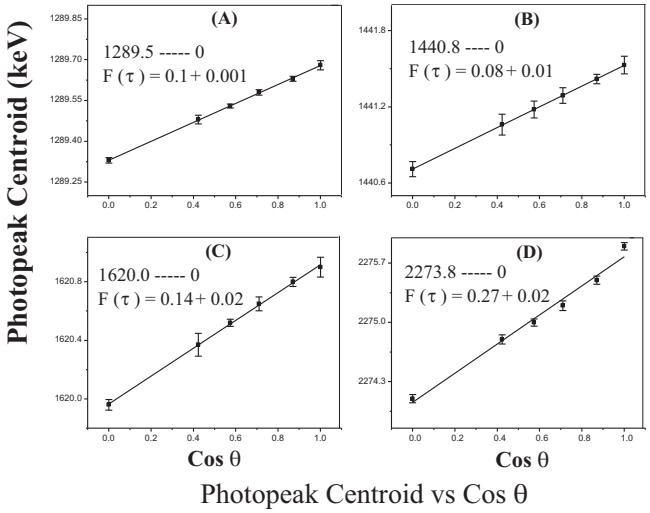

Fig. 3. The plots of photopeak centroid energies of the indicated transitions *versus* $\cos\theta$. The values of $F(\tau)$ are also reported.

lifetimes were determined using the Doppler Shift Attenuation (DSA) method from the singles gamma-ray spectra obtained at various angles between 0° and 90°. The plots of the centroids of the photo peaks at different angles *versus* cos θ for four transitions are shown in fig. 3. The straight line represents the least square fit. The experimental values of the attenuation factors $F(\tau)$ for various gamma-rays were calculated from the slope of the straight lines which were the plots of E_θ *vs.* Cos θ. These straight lines were obtained from the least square fits to the experimental data, using the relation

$$E_\theta = E_{90}[1 + \beta(0)F(\tau)\mathrm{Cos}\theta],$$

Table 2. Experimental $F(\tau)$ values and mean lifetimes of the levels in ^{53}Mo.

Level (keV)	γ – ray (keV)	Mean Expt. F(τ)	Lifetimes			
			Present (fs)	Ref. [9] (fs)	Ref. [14] (fs)	Ref. [33][(a)] (ps)
1289.5	1289.5 911.8	0.1 ± 0.002	472 ± 25	810 ± 300	550 ± 40	4.82
1440.8	1440.8	0.08 ± 0.01	600 ± 55	810 ± 250	600 ± 80	2.05
1620.0	1620.0 1242.1	0.14 ± 0.02	326 ± 45	660 ± 200	480 ± 60	1.11
2273.8	2273.8 1896.5 984.0	0.27 ± 0.02	152 ± 31	470 ± 135	250 ± 50	0.02

[(a)] Theoretical values.

Table 3. $B(E2)$ and $B(M1)$ values for low-energy states in ^{53}Mn. The excitation energy E_x is shown in keV.

Initial $J^\pi(E_x)$	Final $J^\pi(E_x)$	Multipole	Present (W.u.)	Experimental (W.u.) [20,34]	Theoretical (W.u.) [34]
$3/2^-$ (1289.5)	$5/2^-$ (377.7)	$M1$	0.0390(34)	0.023	0.0194
		$E2$	3.3(8)	1.9(5)	0.6
	$7/2^-$ (0.0)	$E2$	22.2(19)	13.4(11)	8.1
$11/2^-$ (1440.8)	$7/2^-$ (0.0)	$E2$	18.5(2)	12.8(18)	9.4
$9/2^-$ (1620.0)	$5/2^-$ (377.7)	$E2$	7.1(1)	3.7(6)	3.6
	$7/2^-$ (0.0)	$M1$	0.0025(4)	0.0012(3)	0.0002
		$E2$	15.1(2)	7.0(9)	5.4
$5/2^-$ (2273.8)	$3/2^-$ (1289.5)	$M1$	0.0049(18)	0.0021(8)	0.0000
		$E2$	7.1(1)	3.0(15)	0.0
	$5/2^-$ (377.7)	$M1$	0.044(6)	0.0019(4)	0.0010
		$E2$	1.5(4)	0.61(14)	1.6
	$7/2^-$ (0.0)	$M1$	0.013(26)	0.0054(11)	0.0023
		$E2$	0.2(1)	0.07(4)	0.02

where E_θ is energy of gamma-ray at an angle θ w.r.t. beam direction and $\beta(0)$ is the velocity of recoiling nucleus in the forward direction along the beam axis.

The adopted experimental $F(\tau)$ denotes the average of the $F(\tau)$ values for all the observed transitions from the same level. The value of theoretical $F(\tau)$ were obtained using Lindhard, Scharff and Schiott theory [29] for stopping power along with the Blaugrund correction [30]. The nuclear stopping power as well as electronic stopping power were used in this analysis. The details of the DSAM analysis are given in the earlier publications [31,32] from our Cyclotron laboratory. The gamma-ray energies, the mean experimental $F(\tau)$ values and the mean lifetimes of the levels are shown in table 2. The comparison of mean lifetimes with previously reported values [9,14,33] is also given in table 2. The reduced transition probabilities $B(M1)$ and $B(E2)$ extracted from the measured values of lifetimes in the present study and the multipole mixing ratios from refs. [9,20] are compared with the single particle estimates and previously reported experimental [20, 34] and theoretical values in table 3.

4 Discussion

The level energies and the gamma-transitions in ^{53}Mn nucleus measured in the present work are given in table 1. The branching ratios for various transitions are compared

with the reported values [9,11,28] and almost all the values are in close agreement with the corresponding reported experimental results. Table 2 gives the present and previously reported experimental and theoretical values of lifetimes of the four levels at 1289.5, 1440.8, 1620.0 and 2273.8 keV excitation energies. The deduced $B(M1)$ and $B(E2)$ reduced transition probabilities for various transitions are compared with the reported [20,34] experimental and theoretical values in table 3. A detailed discussion about the results of these levels is given below.

4.1 Comparison with other experimental works

4.1.1 The 1289.5 keV level

This level was observed to decay through two transitions $1289.5 \rightarrow 0$ (1289.5 keV) and $1289.5 \rightarrow 377.7$ (911.8 keV). The present branching ratios are in agreement with the results of Goodman and Donahue [9]. The lifetime of this level was found to be 472 ± 25 fs, which is in close agreement with the reported values [9,14]. The $B(E2)$ values for 911.8 and 1289.5 keV transitions were obtained using the present results 3.3 ± 0.8 and 22.2 ± 19 W.u. The first transition is a mixed transition with $B(M1)$ value of 0.0390 (34) W.u. The previously reported [20,34] respective $B(E2)$ values are 1.9 (5) and 13.4(11) W.u. The reported value of $B(M1)$ for the mixed 911.8 keV transition is 0.023 W.u. The present results are in satisfactory agreement with the values reported in literature. The ground and the 1289.5 keV states seem to have stronger collective character than the 377.7 keV state.

4.1.2 The 1440.8 keV level

This level has been reported to decay through a single transition to ground state [9]. The present data confirms the decay mode via the $1440.8 \rightarrow 0$ (1440.8 keV) transition. The lifetime of this level as measured in the present experiment is 600 ± 55 fs. The $B(E2)$ value is obtained using the present lifetime result as 18.5 ± 2 W.u. for the 1440.8 keV transition. Due to the predominantly collective nature of this level, we assume a pure quadrupole character for the transition to the ground state. The present $B(E2)$ value is in reasonable agreement with the previous results of 12.8(18) W.u. [20,34].

4.1.3 The 1620.0 keV level

This level is found to decay through $1620.0 \rightarrow 0$ and $1620.0 \rightarrow 377.7$ keV transitions with branching ratios of $84.2 \pm 2.0(\%)$ and $15.8 \pm 1.8(\%)$, respectively. In the previous data, the first transition is also shown much stronger than the second transition. The lifetime of this level has been measured in the present experiment as 326 ± 45 fs. The previously measured $B(E2)$ value for the 1620.0 377.7 keV transition is 3.7(6) W.u., while the reported values of $B(E2)$ and $B(M1)$ for the mixed ground state transition are 7.0(9) and 0.0012(3) W.u., respectively. The present results are in reasonable agreement with the previous reported data. The results suggest that the transition from 1620.0 keV state to ground state is more collective in nature than the transition to 377.7 keV state.

4.1.4 The 2273.8 keV level

This level decays via three transitions, one to ground state and the others to the 377.7 and 1289.5 keV states with branching ratios of 80.9%, 18.0% and 1.1%, respectively. The third transition has not been observed in the previous experiments [9,11]. The measured lifetime of this level is 152 ± 31 fs shorter than the previously measured value [14]. The transition rates are calculated from the presently measured lifetime and are given in table 3. All the three transitions from this level are mixed in character. The previously reported [20,34] $B(E2)$ and $B(M1)$ transition probabilities are in satisfactory agreement with the present results. These results suggest that the 2272.8 keV level has a predominant single particle character.

4.2 Theoretical interpretation

In the fp-shell semi-magic nucleus ^{53}Mn ($N = 28$, $Z = 25$), the protons and neutrons occupy the same major shell. The proton and neutron interaction is thus relatively strong resulting into collective effects, such as $T = 0$ pairing. So in fp shell orbitals $1f_{7/2}$, $2p_{3/2}$, $1f_{5/2}$ and $2p_{1/2}$, one finds the interplay of collective and single particle properties which can be described within a unified framework by the shell model. The effective interaction is a key ingredient for the success of the nuclear shell model. The unified effective interaction Hamiltonian as defined by Honma *et al.* [34], is decomposed into the monopole part HM, which describes bulk properties such as average energy of eignstates in a given configuration, and the multipole part HM, which is dominated by several terms such as pairing, and the quadrupole —quadrupole interaction which determines collective properties of the effective interaction. For shell model calculations for ^{53}Mn, one assumes ^{58}Ni as an inert closed core, and essentially the full set of fp-configuration and the associated unified interaction in order to describe various nuclear properties. The ^{53}Mn nucleus is described in terms of ^{56}Ni closed shell configurations, plus three proton holes in the $1f_{7/2}$ orbit. So the experimental results on the low-lying states of ^{53}Mn have been explained by the $\pi(1f_{7/2})^{-3}$ configuration in a spherical shell model basis. Under such an assumption the ground state $7/2^-$ (0.0) and the first-through-fifth excited states with $5/2^-$ (377.7), $3/2^-$ (1289.5), $11/2^-$ (1440.8), $9/2^-$ (1620.0) and $(5/2)^-$ (2273.8) J^π (excitation energies) were fixed, which were satisfactorily reproduced by our measurements. The mean lifetimes of the second-through-fifth excited levels and the $B(E2)$ and $B(M1)$ values were calculated by Honma *et al.* [34]. For the first four states, which are low spin Yrast states, the lowest $(f_{7/2})^{13}$ configuration is dominant (46 to 60%) in the calculated wave functions.

The non-Yrast state $(5/2)^-$ (2273.8 keV) contains a large amount of multiparticle (neutron) excitations from the $N = 28$ core. The general configuration of $(5/2)^-$ non-Yrast state is $\nu(f_{7/2})^7\ (r)$, where r stands for ($p_{3/2}$, $f_{5/2}$, $p_{1/2}$). In this level the main configuration is 1p-1h type (about 60%) plus other broken core components such as 3n-3h (17%) + 4n-4h ($\sim$ 6%). The effective interaction shell model calculations [34] for electromagnetic transition probabilities are compared with experimental data. Reasonable agreement seen in most cases suggests that the effective interaction shell model description is quite satisfactory.

5 Summary and conclusions

The branching ratios for the gamma decay of the first five excited states $5/2^-$ (377.7), $3/2^-$ (1289.5), $11/2^-$ (1440.8), $9/2^-$ (1620.0) and $(5/2)^-$ (2273.8) keV of ^{53}Mn, the mean lifetimes of second-through-fourth excited levels were determined and the $B(E2)$ and $B(M1)$ values for various transitions were obtained. The present results are in satisfactory agreement with previously reported results [20,34]. The results suggest that while $5/2^-$ (2273.8 keV) level has a dominant single particle character, the $5/2^-$ (377.7 keV) level also manifests only weak collective nature, while the other three levels are dominantly collective in character. The interpretation of data in terms of effective interaction shell model calculations reveals that while other observed low-lying levels which are Yrast states and can be expressed in terms of $\pi(f_{7/2})^{-3}$ configuration. The $(5/2)_2^-$ level is non-Yrast with wave function involving a large amount of multiparticle (neutrons) excitations from the $N = 28$ core.

The authors thank the technical staff of Cyclotron laboratory for providing an excellent proton beam for the experiment. The financial support from CSIR in the form of a research project (KPS) is gratefully acknowledged.

References

1. J.N. Black, Wm.C. McHarris, W.H. Kelly, B.H. Wildenthal, Phys. Rev. C **11**, 939 (1975).
2. W.H. Chung, D.M. Sheppard, W.C. Olsen, B.C. Roberston, Can. J. Phys. **51**, 1840 (1973).
3. P.G. Kerr, S.A. Wender, J.A. Cameron, Nucl. Phys. A **226**, 381 (1974).
4. S.H. Sie, G.G. Frank, H.C. Evans, Nucl. Phys. A **243**, 1 (1975).
5. G.U. Din, I.A. Al-Agil, A.M.A. Al-Soraya, Phys. Rev. C **44**, 972 (1991).
6. I. Fodor, J. Sziklai, P. Klienwachter, H. Schobbert, F. Hermann, J. Phys. G **5**, 1267 (1979).
7. P. Kleinwachter, H.U. Gersch, H. Schobbert, Nucl. Phys. A **398**, 476 (1983).
8. Y. Ozawa, Y. Oguri, E. Atai, Nucl. Phys. A **440**, 13 (1985).
9. A.S. Goodman, D.J. Donahue, Phys. Rev. C **5**, 875 (1972).
10. P. Banerjee, B. Sethi, M.B. Chatterjee, R. Goswami, Phys. Rev. C **44**, 1128 (1991).
11. P. Fintz, I. Riedinger-Ordonez, G. Guillaume, F. Jundt, A. Gallmann, J. Phys. (Paris) **40**, 511 (1979).
12. K.A. Aniol, D.W. Gebbie, C.L. Hollas, J. Nurzynski, Nucl. Phys. A **303**, 154 (1978).
13. Z.P. Sawa, Phys. Scr. **7**, 5 (1975).
14. P.D. Georgopulos, E.J. Hoffman, D.M. Van Patter, Nucl. Phys. A **226**, 1 (1974).
15. J.E. Park, W.W. Daehnick, M.J. Spisak, Phys. Rev. C **19**, 42 (1979).
16. S. Gales, S. Fortier, H. Laurent, J.M. Maison, J.P. Schapira, Phys. Rev. C **14**, 842 (1976).
17. C.J. Lister, J.W. Olness, Phys. Rev. C **18**, 2169 (1978).
18. Isao Kohno, Kenji Katori, Takashi Mikumo, T. Motobayashi, S. Nakajima, M. Yoshie, H. Kamitsubu, J. Phys. Soc. Jpn **42**, 1 (1977).
19. B.R. Fulton *et al.*, Nucl. Phys. A **315**, 477 (1979).
20. Huo Junde, Nucl. Data Sheets **110**, 2869 (1999).
21. A.G.M. Van Hees, P.W.M. Glaudemans, Z. Phys. A **303**, 267 (1981).
22. R.B.M. Mooy, P.W.M. Glaudemans, Z. Phys. A **312**, 59 (1983).
23. Hitoshi Nakada *et al.*, Nucl. Phys. A **571**, 467 (1994).
24. T. Kakavand, K.P. Singh, I.M. Govil, Acta Phys. Pol. B **30**, 2767 (1999).
25. T. Kakavand, K.P. Singh, Int. J. Mod. Phys. E **11**, 347 (2002) **11**, 463(E) (2002).
26. K.P. Singh, Tayeb Kakavand, Mumtaz Oswal, Ashok Kumar, B.R. Behera, Gulzar Singh, *Indian Particle Accelerator Conference (InPAC2006) November 1-4, 2006* (ISPA, 2006).
27. J. Singh, R. Singh, D. Mehta, P.N. Trehan, DAE Nucl. Phys. Symp. B **37**, 455 (1994).
28. I.M. Szoghy, B. Cujec, R. Dayrus, Nucl. Phys. A **153**, 529 (1970).
29. J. Lindhard *et al.*, Mat. Fys. Medd. Dan Vid Selsk **33**, 14 (1963).
30. A.E. Blaugrund, Nucl. Phys. **88**, 501 (1966).
31. V.K. MIttal, D.K. Avasthi, I.M. Govil, J. Phys. G **9**, 91 (1983).
32. K.C. Jain, S.S. Datta, D.K. Avasthi, V.K. MIttal, I.M. Govil, Phys. Rev. C **35**, 534 (1987).
33. K. Lips, Phys. Rev. C **4**, 1482 (1971).
34. M. Honma, T. Otsuka, B.A. Brown, T. Mizusaki, Phys. Rev. C **69**, 034335 (2004).